

Low Temperature Production of Formaldehyde from Carbon Dioxide and Ethane by Plasma-Assisted Catalysis in a Ferroelectrically Moderated Dielectric Barrier Discharge Reactor

Ana Gómez-Ramírez,^{†,⊥} Víctor J. Rico,[†] José Cotrino,^{†,‡} Agustín R. González-Elipe,[†] and Richard M. Lambert^{*,†,§}

[†]Laboratory of Nanotechnology on Surfaces. Instituto de Ciencia de los Materiales de Sevilla (CSIC-Uni. Sevilla), Avda. Américo Vespucio 49, 41092 Sevilla, Spain

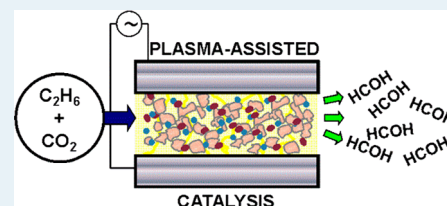
[‡]Departamento de Física Atómica, Molecular y Nuclear, Uni. Sevilla, Avda. Reina Mercedes, 42022 Sevilla, Spain

[§]Chemistry Department, Cambridge University, Cambridge CB2 1EW, United Kingdom

Supporting Information

ABSTRACT: Plasma-assisted catalysis of the reaction between CO₂ and C₂H₆ in a single-pass, ferroelectrically moderated dielectric barrier discharge reactor has been studied at near ambient temperature as a function of physicochemical and electrical reaction variables. The presence of small amounts of a vanadia/alumina catalyst dispersed on the BaTiO₃ ferroelectric markedly enhanced the production of formaldehyde, the focus of this work. A maximum HCOH selectivity of 11.4% (defined with respect to the number of ethane carbon atoms consumed) at ~100% ethane conversion was achieved, the other products being CO, H₂O, H₂, CH₄ and a small amount of C₃H₈. N₂O was also an effective partial oxidant (HCOH selectivity 8.9%) whereas use of O₂ led to complete combustion, behavior that may be rationalized in terms of the electron impact excitation cross sections of the three oxidants. Control experiments with the coproducts CH₄ and C₃H₈ showed that these species were not intermediates in HCOH formation from C₂H₆. Analysis of reactor performance as a function of discharge characteristics revealed that formaldehyde formation was strongly favored at low frequencies where the zero-current fraction of the duty cycle was greatest, the implication being that plasma processes also acted to destroy previously formed products. A tentative reaction mechanism is proposed that accounts for the broad features of formaldehyde production.

KEYWORDS: plasma-assisted catalysis, CO₂+C₂H₆, formaldehyde, ferroelectric moderator, dielectric barrier discharge



1. INTRODUCTION

The energy-efficient conversion of lower alkanes, especially CH₄ and C₂H₆, the principal components of natural gas, into added-value oxygenates is difficult and demanding. Conventional heterogeneous catalysis using supported metal oxides in the presence of a gaseous oxidant has often been used in the research laboratory for the production of C1 and C2 aldehydes from CH₄ and C₂H₆, with varying degrees of success. However, this approach necessarily involves the application of temperatures in excess of 600 °C (see, for example, reference 1 and references therein). With respect to industrial significance, formaldehyde is an important high volume product in the global economy, widely used in the chemical industry and in construction, wood processing, furniture manufacture and textiles: the annual global rate of production being in the order of 12 000 kilotons.² Although laboratory scale Mo oxide-catalyzed oxidation of ethane to formaldehyde has been reported, see for example,³ temperatures in the order of ~600 °C are required. Current commercial process technology involves high temperature heterogeneous catalytic oxidation of methanol over Ag or oxides of Fe, Mo or V. This is a multistep route, first requiring hydrocarbon reforming, followed by

methanol synthesis, and finally formaldehyde production. The alternative one-step route via direct oxidation of light hydrocarbons is not industrially viable because formaldehyde is more readily oxidized than the hydrocarbon reactants under the high temperatures required.²

Plasma-assisted heterogeneous catalysis has often been used as a means for the destruction of a variety of pollutants at low temperatures^{4–6} and a comprehensive review of such work is provided in.⁷ However, this approach has seldom been explored for synthetic processes aimed at chemicals production.

We have previously reported on plasma reforming of hydrocarbons in the absence of a conventional solid catalyst but with BaTiO₃, a ferroelectric material, incorporated in the plasma excited volume.^{8–10} In every case, 100% selective conversion to CO + H₂ was achieved, the ferroelectric serving to markedly reduce the operating voltages required, thus increasing overall energy efficiency. Here we report on the plasma-assisted selective oxidation of ethane to formaldehyde

Received: September 24, 2013

Revised: December 18, 2013

Published: December 20, 2013

by CO₂ in the presence of both a ferroelectric and an appropriate catalyst. Encouraging results are obtained which demonstrate that formaldehyde can be produced at useful selectivity in a single pass atmospheric pressure reactor at high reactant conversion and near ambient temperature.

2. EXPERIMENTAL METHODS

2.1. Dielectric Barrier Reactor. The dielectric barrier discharge (DBD) reactor has been described in detail elsewhere.⁸ It consisted of two concentric stainless steel cylindrical electrodes with diameters of 15 and 36 mm and 115 cm overall length. The interelectrode gap was filled with ~200 g of 2–4 mm BaTiO₃ pellets (Alfa Aesar) with dielectric constant 1250–10 000 over the temperature range 20–120 °C. This ferroelectric material enabled the discharge to be sustained at much lower applied voltages (i.e., from approximately 1.2 to 3 kV for a separation between the electrodes of 1.05 cm). Glass beads (~10% by volume) were incorporated in the interelectrode space to prevent the compaction of the ferroelectric material. These enabled a more homogeneous distribution of microdischarges, which, for reasons explained below, enhanced the efficiency of chemical conversion. For higher operating frequencies, the applied voltage was limited by the power supply characteristics. The gas lines and the reactor (void volume ~ 60 cm³) were maintained at 120 °C to avoid condensation of water. All experiments were carried out at atmospheric pressure.

The plasma was ignited by a purpose-built bipolar AC power supply incorporating two output transformers (15 kV maximum) each connected to an electrode. This configuration provided voltages of 10–30 kV at frequencies from 750 to 8 kHz. In all experiments, the electrical parameters were monitored by means of a digital oscilloscope (Tektronix TDS 2001C) used to display voltage/current characteristics via a high voltage probe and an inductively coupled current/voltage converter. The overall reactor set up is illustrated in Figure 1.

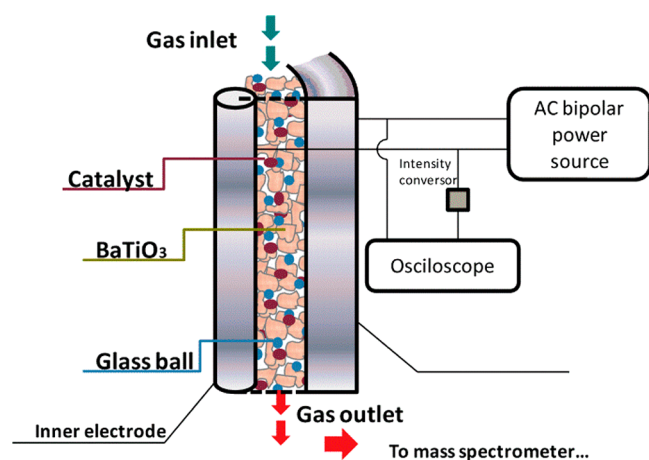


Figure 1. Schematic of the reactor.

In plasma reforming processes, the discharge current and voltage depend on factors including the type of dielectric material and its configuration, pressure, gas composition, interelectrode gap and electrode design.^{11–13} With such reactors, assessment of $I(t)$ and $V(t)$ curves provides useful information about discharge conditions and can be used to predict the efficiency of the reforming processes.¹⁴ Here,

electrical characterization was carried out by varying the frequency from 900 to 7474 Hz at constant applied voltage (peak value 1.8 ± 0.1 kV). Figure 2 shows typical $I(t)$ and $V(t)$

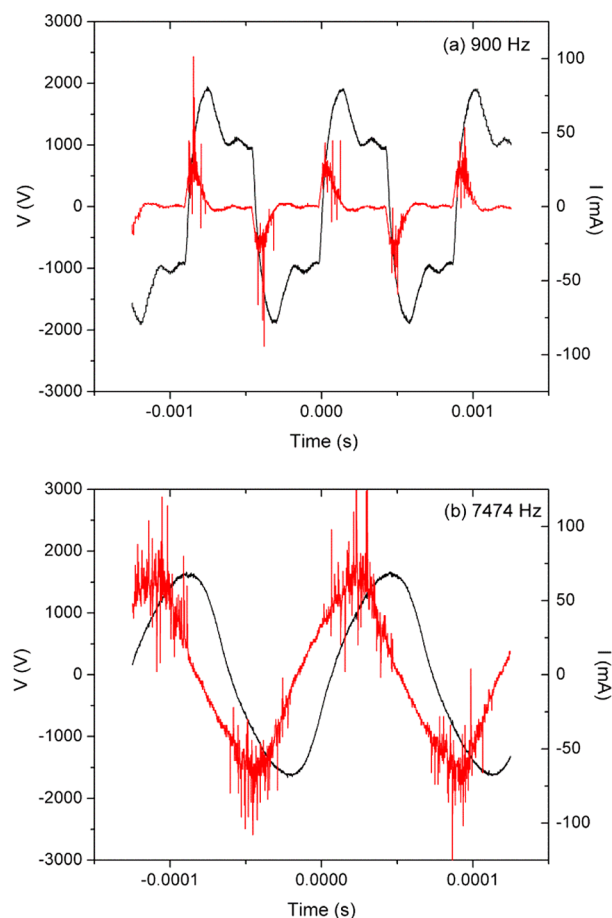


Figure 2. $V(t)$ (black curve) and $I(t)$ (red curve) curves obtained at (a) 900 Hz and (b) 7474 Hz for a nominal applied voltage of 1.8 ± 0.1 kV.

curves recorded at frequencies of 900 and 7474 Hz. Note that at 900 Hz the discharge current is concentrated within a small temporal region whereas at high frequencies the $I(t)$ curves do not reach a zero current regime, a point that we shall return to. The spikes are due to microdischarges that spread over the electrode surface when a high local electric field causes local breakdown of the gas.^{15,16} The presence of solid particles in the discharge volume may modify the system's electrical behavior and performance by promoting surface discharges on these particles.¹⁷

The discharge power (P) can be calculated from the area of the Lissajous curves.¹⁸ This parameter allows estimation of the reaction efficiency defined as σ/P , where σ refers to the amount of C₂H₆ consumed. P was strongly dependent on the operating frequency (ν) and voltage: at fixed voltage, P increased with frequency due to progressively increasing discharge current (see Supporting Information S1).

2.2. Catalyst Preparation. The vanadia/alumina catalyst was prepared according to the method used by Blasco et al.¹⁹ Materials of this type have been widely used as conventional catalysts for oxidative dehydrogenation of ethane, following their introduction many years ago by Thorsteinson et al.^{20,21}

A solution of oxalic acid (30.3 g, Sigma Aldrich) and NH_4VO_3 (24.7 g, Sigma Aldrich) in 100 mL of water was prepared by heating and stirring. Portions of this solution were then added to alumina powder (Sigma Aldrich) to achieve the desired loading of vanadium. After impregnation, the precursor was calcined at 600 °C for 6 h to produce the final catalyst, which contained 1.74% (w/w) of vanadia. The BET specific surface area of the catalyst(s) determined by means of N_2 adsorption, (Micromeritics Tristar II 3020) was 67 m^2/g with a total pore volume of 0.164 cm^3/g and average pore diameter of 7 nm. Small pellets of this catalyst (~1 mm diameter) were fabricated by compressing and then crushing the initially synthesized powder. The catalyst pellets were then mixed with BaTiO_3 pellets (~3 mm in diameter), loaded into the reactor and used to investigate the effects of catalyst loading on the system's performance. The weight ratio catalyst/ferroelectric material was varied from 0 to 2.5×10^{-3} , with 2.5×10^{-3} being used in most experiments as standard operating conditions.

XRD revealed that the used catalyst was amorphous and XPS showed that the vanadium was present as V^{5+} . The corresponding Raman spectra were uninformative, which is perhaps unsurprising, given that the catalyst constituted only a small component of the mixture with BaTiO_3 . However, SEM images and corresponding EDX spectra were revealing. They clearly showed the two components of the BaTiO_3 /catalyst composite and demonstrated that the vanadia was exclusively associated with the alumina phase. A representative image and spectra are shown in the Supporting Information (S2).

2.3. Gas Delivery and Analysis of Reactor Output.

Gases were delivered to the reactor by means of mass flow controllers (Bronkhorst, EL-flow type); ethane and CO_2 , O_2 , N_2O , He, Ar, N_2 supplied by Air Liquide were used without purification and the gas composition at the reactor exit was monitored mass spectrometrically (Sensorlab, Prima Plus–Pfeiffer Vacuum). Gas mixtures of known composition were used to calibrate the quadrupole mass spectrometer (QMS), thus enabling quantification of reaction products. In the case of formaldehyde, we used the QMS sensitivity factor directly determined by Mensch, whose sensitivity factors for CO, CO_2 , CH_4 and H_2 are very similar to ours.²² The m/z values used to quantify each of the products and reactants were as follows: C_2H_6 $m/z = 27$, CO_2 $m/z = 44$, CO $m/z = 28$, CH_4 $m/z = 15$, C_3H_6 $m/z = 39$, H_2O $m/z = 18$, COH_2 $m/z = 29$.

Unless otherwise stated, the following standard flow conditions were used: 5.9 sccm CO_2 ; 1.1 sccm C_2H_6 ; 27.1 sccm He. (He is often used as carrier gas as it favors the attainment of homogeneous glow discharge conditions²³). In the cases of formaldehyde and methane, quoted selectivities are calculated relative to the number of ethane carbon atoms consumed.

For the other products (H_2 , H_2O , CO), which may arise from either or both reactants, the absolute effluent flow rates are given in sccm.

3. RESULTS AND DISCUSSION

Under most operating conditions, the plasma-assisted catalytic system converted essentially all the C_2H_6 in a single pass accompanied by substantial net conversion of CO_2 (which is itself a reaction product). The principal products were H_2 , H_2O , CO, CH_4 and, most significantly, formaldehyde (HCOH). Selectivity toward formation of the latter was as high as 11.4% (0.24 sccm) under some conditions. Very small amounts of C_3H_8 were also observed.

We now examine the effect of operating parameters, including the catalyst, on the selectivity toward HCOH production and on the energy efficiency of the process. On the basis of these results, a hypothesis will be proposed to account for the formation of HCOH by plasma-assisted catalysis.

3.1. HCOH Production: Effect of Discharge Parameters.

Figure 3a,b shows the evolution of reactants and products

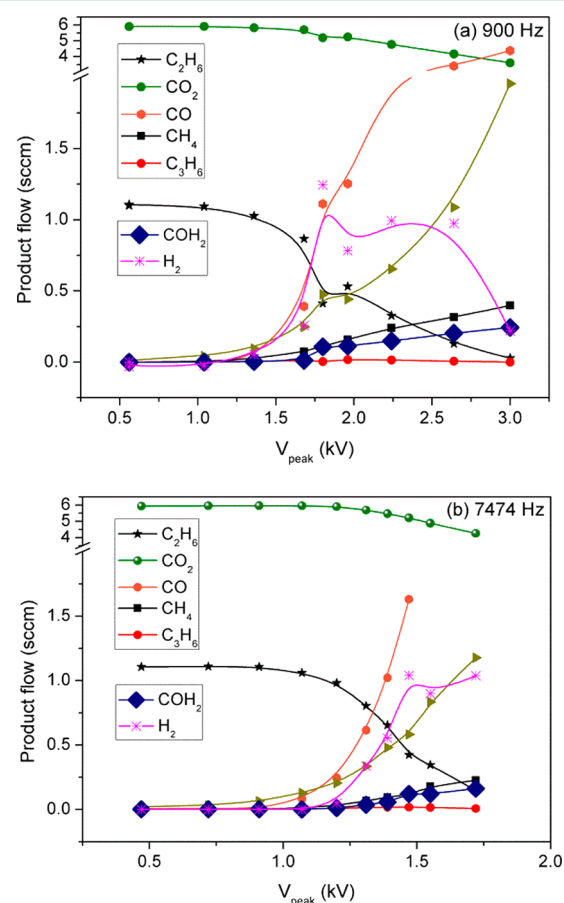


Figure 3. Evolution of reactant and product outflow as a function of applied voltage for (a) 900 Hz, (b) 7474 Hz. See also Table S3.1 in the Supporting Information. At high frequencies, the applied voltage was limited to 1.8 kV by the power supply.

expressed in terms of sccm as a function of applied voltage for the minimum and maximum accessible frequency values. At intermediate frequencies, the results lay between those illustrated in Figure 3a,b. These results are also presented in tabular form in the Supporting Information (S3).

The most striking finding is the formation of substantial amounts of HCOH and methane at all operating frequencies, accompanied by very small amounts of C_3H_8 . These results constitute the first demonstration that a valuable oxygenate can be obtained with relatively high selectivity in a plasma-assisted catalytic process at near ambient temperature. It might reasonably be expected that substantial improvements in performance could be achieved by optimizing reactor design and the associated operating parameters, which will be the basis for further studies. At the lowest frequency (Figure 3a, 900 Hz), formaldehyde production increased from zero sccm (no discharge) to 0.244 sccm at 3 kV, equivalent to a selectivity of 11.4%; the corresponding methane selectivity was 18.6%

(0.39 sccm). At 7474 Hz and 1.8 kV, the HCOH and CH₄ equivalent selectivities were 8.5% and 11.9% (0.16 and 0.23 sccm), respectively.

CO, H₂ and H₂O were formed in larger amounts, the yield of CO increased continuously with applied voltage while that of H₂ exhibited a maximum at ~1.8 kV at 900 Hz and ~1.5 kV at 7474 Hz. The decrease in H₂ production was likely due to increasing formation of H₂O.

In a plasma-assisted catalytic system, both plasma and surface reactions are expected to contribute to the product distribution, a topic that we consider below. An indication of the relative importance of purely plasma reactions in formaldehyde formation may be obtained by referring HCOH flow to plasma power. This is exemplified in Table 1, which shows C₂H₆

Table 1. Dependence of Reactant Conversion and Formaldehyde Production on Discharge Frequency and Power for a Nominal Applied Voltage of 1.8 ± 0.1 kV

ν (Hz)	P (w)	σ (sccm)	σ/P (sccm·w ⁻¹)	HCOH flow/ P (sccm·w ⁻¹)
900	4.80	0.697	0.145	0.0229
4000	12.32	0.786	0.064	0.0089
5500	23.60	0.860	0.036	0.0056
7474	24.44	0.958	0.039	0.0067

converted and HCOH flow produced as a function of frequency and discharge power at a constant voltage of 1.8 kV. The fourth and fifth columns show that although reactant conversion increases markedly with frequency (and power), the efficiency toward both conversion and HCOH production decreases very strongly with increased frequency. A compilation of data for CH₄ and HCOH production and selectivities for other frequencies and voltages is given in the Supporting Information, along with corresponding data for the other products (see Supporting Information S3).

In this regard, the profile of the $I(t)$ and $V(t)$ curves in Figure 2 is revealing. Maximum energy efficiency toward the desired chemistry is obtained at low frequencies. This strongly suggests that the effect is linked to the zero current fraction of the duty cycle (~60% at 900 Hz and ~0% at 7474 Hz). Purely plasma processes can both activate reactants (see below) and also destroy previously formed products. For any given reaction product, the balance between these two effects will determine the net reaction yield. In the present case, it appears that net HCOH production is disfavored by destructive secondary reactions that occur while the plasma is lit.

It is also likely that the relative importance of micro-discharges versus surface discharges in determining overall reaction efficiency is frequency dependent.¹⁷ These findings signpost future developments whereby reaction selectivities may be substantially increased by suitably engineering both the reactor geometry and the electrical characteristics of the discharge.

For a frequency of 900 Hz, Figure 4 shows the voltage dependence of reaction efficiency (i.e., product flow or reactant consumption per unit injected power) for ethane consumption and formation of the various products. At 7474 Hz, the efficiency was much lower, for reasons discussed below, and corresponding results are presented in the Supporting Information (S4).

In all cases, the efficiency exhibits a pronounced maximum at ~1.8 kV, suggesting the occurrence of a plasma resonance at around this operating voltage.⁷

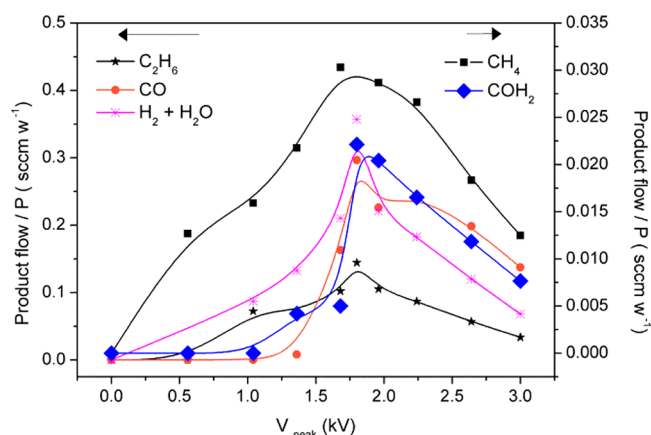


Figure 4. COH₂ and CH₄ process efficiency (flow (sccm)/ P) and CO, H₂ + H₂O and C₂H₆ flows referred to the applied power as a function of the reactor voltage ($\nu = 900$ Hz). The C₂H₆ curve refers to the consumption of this reactant.

The decline in efficiency at higher voltages suggests that the more active plasma discharges obtained under such conditions induce undesired side reactions and/or further conversion of the desired product. The slower decline in CO production compared to the other products for $V > 1.8$ kV suggests that secondary reactions that convert HCOH and/or CH₄ into CO are responsible for the observed behavior. Similar results were obtained at higher frequencies (see Supporting Information S4 for $\nu = 7474$ Hz).

3.2. HCOH Production: Effect of Gas Composition and Catalyst Load. To obtain additional insight into the reaction mechanism, especially with respect to formation of HCOH, the use of O₂ and N₂O as alternative oxidants was investigated. Likewise, the effects of using Ar and N₂ as carrier gases and the use of methane and propane as alternative reactants were also studied. Experiments were carried out under the standard conditions defined above, and Table 2 summarizes the results. Uncertainties in the CO yield, estimated as described below, are given in the final column.

In the cases of C₂H₆ + CO₂ with Ar, N₂ or He, to calculate the CO yield, the $m/z = 28$ signal had to be corrected for the contribution from ethane, CO₂ and HCOH and the associated carbon balances are shown in Figure 5 for the case of He. At 900 Hz, for voltages above 2 kV, the apparent carbon balance closed within the experimental uncertainty; at lower voltages, for both 900 and 7474 Hz, the data were such that the estimated errors in the CO yield expanded rapidly, precluding estimation of the carbon balance, as indicated in the figure. Because measurements were always made at steady state, we conclude that no accumulation of carbon within the reactor could have been occurring.

When N₂ was the carrier gas, the very large contribution to $m/z = 28$ from N₂ had also to be allowed for. This was done by also measuring the $m/z = 14$ signal, which has a significant contribution from N₂, a negligible contribution from CO and small contributions from ethane and methane. Thus, knowing the fragmentation patterns of all three species as measured with our mass spectrometer, it was possible to estimate the CO yield in this case also, though inevitably, the associated error was large. In the case of N₂O as oxidant, CO₂ is a product of reaction. The mass interferences between N₂O, CO₂ and CO are such that the only signal unambiguously ascribable to CO₂ is $m/z = 22$ (CO₂²⁺), which appears only very weakly. Using

Table 2. Effect of Oxidant and Carrier Gas on Reactant Conversion and Product Selectivities (3 kV)^a

gas composition		conversion %		selectivity %		flow (sccm)		
		CO ₂	C ₂ H ₆	COH ₂	CH ₄	H ₂	H ₂ O	CO
1.1 sccm C ₂ H ₆ 5.9 sccm CO ₂	Ar	32.2	92.1	6.7	13.9	1.18	1.16	3.4 ± 0.5
	N ₂	23.2	79.0	11.7	11.8	0.92	1.03	1.5 ± 1.9
	He	39.0	97.8	11.4	18.6	0.22	1.96	4.4 ± 0.6

^aData for O₂ as oxidant not shown as only complete combustion occurred in that case.

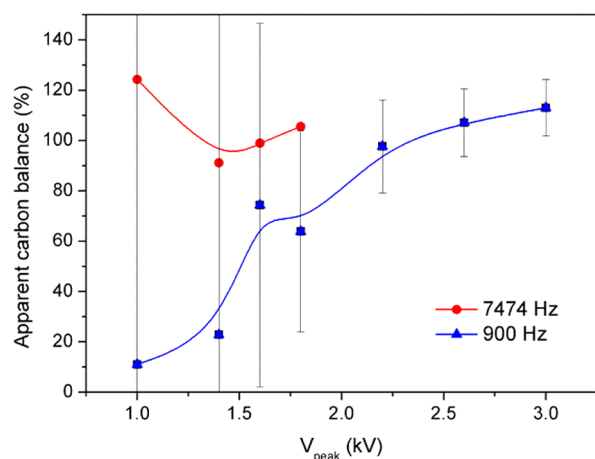


Figure 5. Apparent carbon balance (%) as a function of the voltage at two frequencies (carrier gas: He).

this as a basis for estimating the amount of CO₂ formed resulted in such a large error that the carbon balance could not be achieved.

It is clear that CO₂ was the most effective partial oxidant, yielding the largest amount of formaldehyde and a comparable amount of methane. Interestingly, when N₂O was used as oxidant, the yield of formaldehyde (8.9%) was only slightly smaller than that obtained with CO₂, although methane production was drastically reduced (3.2%). On the other hand, using O₂ resulted in the complete combustion of ethane to yield carbon dioxide and water.

Substitution of He by N₂ as carrier gas produced a decrease in methane production, whereas with Ar as carrier gas, both formaldehyde and methane production decreased substantially. This correlates with the well-known behavior of He in promoting homogeneous discharges in DBD plasmas due to formation of higher concentrations of high energy long-lived metastable species.²⁴ In the present case, this effect was confirmed by demonstrating that the relative intensity of microdischarges was smallest when using He as carrier gas, again, this is consistent with the view that microdischarges induce undesired chemistry (see Figure 2).

Given the presence of methane and small amounts of propane in the effluent gas, we investigated the possibility that these species could be reaction intermediates in the formation of formaldehyde. Accordingly, we carried out DBD-catalysis reactions with CO₂ + CH₄ and CO₂ + C₃H₈ under experimental conditions similar to those shown in Table 2. With methane, the HCOH selectivity was only 2.2%, even at an overall CH₄ conversion of ~90%. As expected, hydrogen and CO were the main reaction products. With propane, also at a conversion of ~90%, no traces of HCOH were detectable, with CH₄, water, CO and H₂ being the sole reaction products. We therefore conclude that CH₄ and C₃H₈ are unlikely to be important reaction intermediates in the partial oxidation of

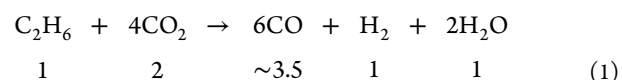
ethane to formaldehyde under conditions of plasma-assisted catalysis.

The influence of catalyst load on reactor performance was also examined by varying the amount of catalyst mixed with the BaTiO₃ from 0 to 0.5 g. The amount of catalyst was kept very low so as to maintain unchanged the plasma characteristics of the reactor. As noted below, even though present in very small amounts, the catalyst had a very significant influence on HCOH selectivity.

Thus, at the optimum catalyst loading of ~0.2 g, formaldehyde production was increased by a factor of ~3 compared to the catalyst-free case (BaTiO₃ only). Increasing the catalyst loading beyond this value did not increase formaldehyde production. See Supporting Information (S5). Thus, it appears that the vanadia/alumina catalyst plays no significant role in methane production, whereas it is of importance in formaldehyde production, which process is in any case our chief concern, which we now consider.

3.3. Mechanistic Considerations. The complexity resulting from the simultaneous occurrence of gaseous and surface processes taking place in any plasma-assisted catalytic system makes detailed interpretation in terms of reaction mechanism speculative at best. Nevertheless, by observing broad trends, useful indications may be obtained. We may simplify the discussion by first considering the consumption of reactants and yields of major products before proceeding to discuss formaldehyde production, which is our principal focus.

From Figure 2, it is apparent that the maximum consumption of C₂H₆ and CO₂ is in the ratio ~1:2 and at ~2.5 kV, the relative yields of H₂:CO:H₂O are ~1:3:1. Making the simplifying approximation that these five species are the only ones involved, one may formally write a balanced equation as follows:



These apparent stoichiometries may be compared with the observed values for relative consumptions and yields, which are shown beneath eq 1.

The observed values for C₂H₆ consumption and H₂ production are in line with eq 1. The observed CO and H₂O yields and the CO₂ consumption are all about half what would be expected on the basis of eq 1. This may be rationalized in terms of simultaneous occurrence of the water gas shift reaction



which would act to decrease the apparent CO₂ consumption and also decrease the apparent CO and H₂O production. Indeed, the occurrence of side reactions, especially at high voltages, is suggested by the shape of the curves in Figure 3. The decrease in H₂ production that eventually occurs above ~2.6 kV correlates with a rapid increase in H₂O production,

suggesting that hydrogen oxidation becomes increasingly important at high voltages.

Turning now to the process of principal interest, under the most favorable conditions, formaldehyde selectivities in excess of 11% are achieved with CO₂ (N₂O is only slightly inferior as a partial oxidant, mechanistically interesting and relevant, but not of significance from the viewpoint of technical application).

Conventional vanadia-based catalysts are capable of converting ethane/oxygen mixtures to formaldehyde at 600 °C, with very high selectivity (>90%), but at very low conversion (~1%).²⁵ Appreciable amounts of CH₄ are also produced under these conditions.^{26,27} Wada et al. suggested that, in such cases, formaldehyde production involved prior formation of acetaldehyde, whereas Lou et al. concluded that formaldehyde arose from the oxidation of ethylene formed from ethane.¹

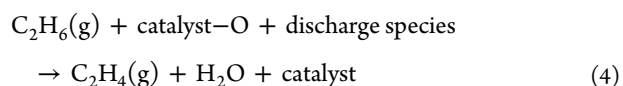
On the basis of these results obtained by conventional high temperature heterogeneous catalysis, we may tentatively propose a surface + gas phase mechanism for low temperature formaldehyde formation under DBD conditions, as observed here, where excited species derived from the plasma are involved in generating active oxygen species on the catalyst surface and also participate in gas phase reactions.

As explained in section 3.2, control experiments were carried out by substituting C₂H₆ by other hydrocarbons to determine whether these molecules could be intermediates in the production of formaldehyde. In neither case was any formaldehyde production detected using He carrier gas with flow and discharge conditions equivalent to those specified in Table 2. These experiments discard that these species are intermediate reactants for the production of formaldehyde. We therefore propose the following reaction scheme, involving both plasma species and surface driven processes with these activated species, as a plausible mechanism for formaldehyde production:

1. Low temperature activation of catalyst by plasma-excited CO₂* species



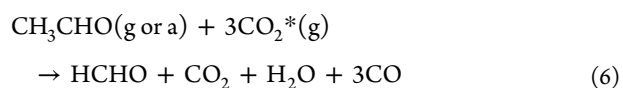
2. Plasma-assisted oxy-dehydrogenation of ethane at the activated oxide surface



3. Gas phase and/or surface catalyzed partial oxidation of ethylene to acetaldehyde by discharge-activated CO₂* molecules



4. Oxidative decomposition of acetaldehyde: the overall process can be formally written as



The above scheme for formaldehyde production is consistent with the high temperature oxidative chemical processes proposed by Lou et al., Wada et al. and Wang et al.^{1,26,27} under conditions of conventional heterogeneous catalysis. Under our conditions, it is envisaged that the oxidative chemistry is carried out at low temperature not by O₂ but by excited CO₂* molecules produced in the discharge but acting

on the surface of BaTiO₃ and more efficiently on that of the catalyst. Recall now that N₂O was nearly as effective as CO₂ in producing formaldehyde, whereas O₂ led only to complete combustion of ethane. These observations are also consistent with the proposed scheme from the point of view of the discharge-induced electron impact excitation of CO₂, N₂O and O₂. Thus, the cross sections for electron impact excitation of CO₂ and N₂O in the range 10–1000 eV are very similar and 1 order of magnitude greater than the corresponding cross section for O₂.²⁸ Thus, in a general sense, given the much greater abundance of excited CO₂ and N₂O species likely present under DBD conditions compared to excited oxygen species, one might expect selective oxygen-transfer reactions such as 1, 3 and 4 to be of comparable importance in the cases of discharges containing CO₂ and N₂O and much less significant in the case of O₂. Finally, note that this proposal is at least consistent with the finding that no formaldehyde production at all was detectable when using either methane or propane instead of ethane, with both CO₂ and N₂O, because the key processes (reaction eqs 2 and 3) are precluded with methane as a reactant and are far less likely when starting with propane because any propene intermediate would undergo rapid combustion rather than selective oxidation due to the presence of allylic hydrogen atoms in the molecule.²⁹ The direct involvement of surface-related processes in formaldehyde production is strongly suggested by the characteristic *I*(*t*) curves in Figure 2, already discussed; species activated in the gas phase react with the activated solid surface and with adsorbed species to yield products that diffuse, desorb and escape or are further modified by secondary gas/surface processes. The latter act to limit net production of formaldehyde, higher frequencies and shorter discharge “off” times therefore lead to reduced formaldehyde yield.

Finally, although it is not our principal interest here, it will be recalled that, under our conditions, methane production is comparable to that of formaldehyde. It seems most likely that ethane is the source of this product. Significant methane production was observed by Chao et al. in their study of high temperature ethane → formaldehyde conversion by means of conventional heterogeneous catalysis, although no explanation for its formation was offered.²⁵ The fact that methane formation, in contrast with formaldehyde production, is insensitive to the presence of catalyst suggests that CH₄ is formed principally by gas phase processes. Given that the main dissociative channels for electron impact reactions of ethane at energies pertinent to plasma conditions yield, variously, CH₄ + CH₂, CH₃ + CH₃, CH₄ + CH₂⁺ and CH₃ + CH₃⁺³⁰ one may speculate that under DBD conditions, methane production arises from electron impact-induced gaseous reactions of ethane that yield radicals and ions which react further by hydrogen abstraction to form methane.

4. CONCLUSIONS

Partial oxidation by CO₂ of ethane to formaldehyde in a ferroelectrically moderated single-pass DBD reactor yields up to 11.4% formaldehyde at ~100% ethane conversion at near ambient temperature.

The presence of a small amount of vanadia/alumina catalyst dispersed on the ferroelectric phase substantially increases formaldehyde production.

Control experiments indicate that the coproducts CH₄ and C₃H₈ are not intermediates in formaldehyde formation.

Analysis of reactor performance as a function of discharge frequency indicates that formaldehyde production is favored by maximizing the zero current fraction of the duty cycle. This implies that in addition to providing the necessary activation of the system, the plasma also produces unwanted destructive secondary reactions, which take place while the plasma is lit, thus limiting the overall desired chemistry.

Subject to plausible assumptions, a tentative reaction scheme may be devised that accounts for the main features of the system.

The present findings are encouraging and suggest future developments whereby reaction selectivities may be substantially increased by suitably engineering both the reactor geometry and the electrical characteristics of the discharge.

■ ASSOCIATED CONTENT

● Supporting Information

Effective Intensity and Consumed power. SEM image and EDX spectra of BaTiO₃/catalyst composite. Formation of products at different voltages and frequencies. Process efficiency as a function of voltage for a frequency of 7474 Hz. Influence of catalyst load on formaldehyde and methane production. This material is available free of charge via the Internet at <http://pubs.acs.org>.

■ AUTHOR INFORMATION

Corresponding Author

* Richard M. Lambert. E-mail: rml1@cam.ac.uk

Present Address

[†]Experimentalphysik V, Physikalisches Institut, Bayreuth Universität, 95440 Bayreuth, Germany.

Notes

The authors declare no competing financial interest.

■ ACKNOWLEDGMENTS

We thank the Junta de Andalucía (Projects P12-FQM-2265, TEP08067 and FQM-6900) and the Ministry of Science and Innovation (Project CONSOLIDER CSD2008-00023, MAT2010-21228 and MAT2010-18447) for financial support. The support of Abengoa Research is also acknowledged.

■ REFERENCES

- (1) Lou, Y.; Wang, H.; Zhang, Q.; Wang, Y. *J. Catal.* **2007**, *247*, 245–255.
- (2) Reuss, G.; Disteldorf, A.; Gamer, O.; Hilt, A. Formaldehyde. In *Ullmann's Encyclopedia of Industrial Chemistry*; Wiley-VCH: Weinheim, Germany, 2002.
- (3) Lou, Y.; Zhang, Q.; Wang, H.; Wang, Y. *J. Catal.* **2007**, *250*, 365–368.
- (4) Kirkpatrick, M. J.; Odic, E.; Zinola, S.; Lavy, J. *Appl. Catal., B* **2012**, *117*, 1–9.
- (5) Harling, A. M.; Demidyuk, V.; Fischer, S. J.; Whitehead, J. *Ch. Appl. Catal., B* **2008**, *82*, 180–189.
- (6) Hueso, J. L.; Cotrino, J.; Caballero, A.; Espinós, J. P.; González-Elipe, A. R. *J. Catal.* **2007**, *247*, 288–297.
- (7) Chen, H. L.; Lee, H. M.; Chen, S. H.; Chang, M. B.; Yu, S. J.; Li, S. N. *Environ. Sci. Technol.* **2009**, *43*, 2216–2227.
- (8) Rico, V. J.; Hueso, J. L.; Cotrino, J.; González-Elipe, A. R. *J. Phys. Chem. A* **2010**, *114*, 4009–4016.
- (9) Sarmiento, B.; Brey, J. J.; Viera, I. G.; González-Elipe, A. R.; Cotrino, J.; Rico, V. J. *J. Power Sources* **2007**, *169*, 140–143.
- (10) Rico, V. J.; Hueso, J. L.; Cotrino, J.; Gallardo, V.; Sarmiento, B.; Brey, J. J.; González-Elipe, A. R. *Chem. Commun.* **2009**, 6192–6194.

- (11) Trunec, D.; Brablec, A.; Stastn, F. *Contrib. Plasma Phys.* **1998**, *38*, 435–445.
- (12) Wang, X.; Luo, H.; Liang, Z.; Mao, T.; Ma, R. *Plasma Sources Sci. Technol.* **2006**, *15*, 845–848.
- (13) Meiners, A.; Leck, M.; Abel, B. *Rev. Sci. Instrum.* **2010**, *81*, 113507–8.
- (14) Massines, F.; Gherardi, N.; Naudé, N.; Ségur, P. *Eur. Phys. J. Appl. Phys.* **2009**, *47*, 22805.
- (15) Li, M.; Xu, G.; Tian, Y.; Chen, L.; Fu, H. *J. Phys. Chem. A* **2004**, *108*, 1687–1693.
- (16) Eliasson, B.; Kogelschatz, U. *IEEE Trans. Plasma Sci.* **1991**, *19*, 1063–1077.
- (17) Tu, X.; Gallon, H. J.; Twigg, M. V.; Gorry, P. A.; Whitehead, J. *C. J. Phys. D: Appl. Phys.* **2011**, *44*, 274007–2740017.
- (18) Manley, T. C. *Trans. Electrochem. Soc.* **1943**, *84*, 83–96.
- (19) Blasco, T.; Galli, A.; López Nieto, J. M.; Trifiró, F. *J. Catal.* **1997**, *169*, 203–211.
- (20) Thorsteinson, E. M.; Wilson, T. P.; Young, F. G.; Kasai, P. H. *J. Catal.* **1978**, *52*, 116–123.
- (21) Gärtner, C. A.; van Veen, A. C.; Lercher, J. A. *Chem. Cat. Chem.* **2013**, DOI: 10.1002/cctc.201200966.
- (22) Mensch, M. *MSc thesis*, Virginia Polytechnic Institute: Blacksburg, VA, March 2003.
- (23) Merche, D.; Vandencastele, N.; Reniers, F. *Thin Sol. Films* **2012**, *520*, 4219–4236.
- (24) Massines, F.; Gherardi, N.; Fornelli, A.; Martin, S. *Surf. Coat. Technol.* **2005**, *200*, 1855–1861.
- (25) Chao, Z.; Ruckenstein, E. *J. Catal.* **2004**, *222*, 17–31.
- (26) Wada, K.; Yoshida, K.; Watanabe, Y.; Suzuki, T. *Appl. Catal., A* **1991**, *74*, L1–L4.
- (27) Wang, Y.; Otsuka, K. *J. Catal.* **1997**, *171*, 106–114.
- (28) Anzai, K.; Kato, H.; Hoshino, M.; Tanaka, H.; Itikawa, Y.; Campbell, L.; Brunger, M. J.; Buckman, S. J.; Cho, H.; Blanco, F.; Garcia, G.; Limao-Vieira, P.; Ingolfsson, O. *Eur. Phys. J. D* **2012**, *66*, 36.
- (29) He, J.; Zhai, Q.; Zhang, Q.; Deng, W.; Wang, Y. *J. Catal.* **2013**, *299*, 53–66.
- (30) Janev, R. K.; Reiter, D. *Phys. Plasmas* **2004**, *11*, 780–830.